

## Optical bistability in subwavelength slit apertures containing nonlinear media

J. A. Porto,<sup>1</sup> L. Martín-Moreno,<sup>2</sup> and F. J. García-Vidal<sup>1</sup>

<sup>1</sup>*Departamento de Física Teórica de la Materia Condensada, Facultad de Ciencias (C-V), Universidad Autónoma de Madrid, E-28049 Madrid, Spain*

<sup>2</sup>*Departamento de Física de la Materia Condensada, ICMA-CSIC, Universidad de Zaragoza, E-50015 Zaragoza, Spain*  
(Received 25 March 2004; revised manuscript received 12 May 2004; published 13 August 2004)

We develop a self-consistent method to study the optical response of metallic gratings with nonlinear media embedded within their subwavelength slits. An optical Kerr nonlinearity is considered. Due to the large  $E$  fields associated with the excitation of the transmission resonances appearing in this type of structure, moderate incoming fluxes result in drastic changes in the transmission spectra. Importantly, optical bistability is obtained for certain ranges of both flux and wavelength.

DOI: 10.1103/PhysRevB.70.081402

PACS number(s): 78.20.Ci, 42.65.Pc, 73.20.Mf

Since the appearance of the photonic crystal concept, there has been a strong interest in the optical properties of nano- and microstructured systems. This is due, in part, to the potential applications for small all-optical devices. An interesting possibility is to include some nonlinear elements in the structures,<sup>1-3</sup> which may result in optical switches and gates. Systems based on nonlinear photonic crystals presenting optical bistability have been recently proposed.<sup>4-7</sup> Another promising route for nonlinear optics is to use structured metal films. The enhanced optical transmission phenomenon found in both subwavelength hole<sup>8</sup> and slit<sup>9-14</sup> arrays, and the high local-field enhancements associated with it<sup>15,16</sup>, suggests the possibility of strong nonlinear transmission effects if nonlinear media are embedded in the structure. Recently, photon transmission gated by light of a different wavelength were reported,<sup>17</sup> and the possibility of bistability in enhanced transmission has been mentioned.<sup>18</sup> However, a detailed calculation for such metallic structures containing nonlinear media has not yet been done.

In this paper, we present a theoretical analysis of the transmission properties of a one-dimensional metallic grating with subwavelength slits, filled with a Kerr nonlinear media. As we will discuss below, even this simple system presents interesting optical properties, such as optical bistability for certain ranges of wavelength and incident flux.

In Fig. 1 we show a schematic view of the structure under study. Unless otherwise stated, the chosen parameters of the grating are:  $d=0.75$ ,  $a=0.05$ , and  $h=0.45$   $\mu\text{m}$ . This set of parameters is typical for experimental studies of subwavelength apertures in the optical regime.<sup>19</sup> The slits are supposed to be filled with a Kerr nonlinear media, whose dielectric constant at point  $\vec{r}$  depends on the intensity of the  $E$  field at this point,  $|E(\vec{r})|^2$ ,

$$\epsilon(\vec{r}) = \epsilon_l + \chi^{(3)}|E(\vec{r})|^2, \quad (1)$$

where  $\epsilon_l$  is the value of the dielectric constant at low intensity and  $\chi^{(3)}$  is the third-order susceptibility related to the Kerr effect. Since the change of the dielectric constant is not very large, it is common to approximate the refractive index as  $n(I) = n(0) + n_2 I$ , where  $I$  is the intensity of the optical field (measured in units of energy flux) and  $n_2$  is known as the

Kerr coefficient. This allows us to express the incident flux,  $I_0$ , in units of  $n_2^{-1}$  and the results will be valid for all Kerr materials with the same  $n(0)$ . In what follows, we consider  $n(0) = 1.5$  ( $\epsilon_l = 2.25$ ).

The electromagnetic (EM) properties of these gratings are analyzed by a modal expansion of the electric and magnetic fields. Two simplifications are incorporated into the exact modal expansion: we consider perfect metal boundary conditions and, as the slit width is much smaller than the wavelength, only the fundamental eigenmode in the modal expansion of the EM fields inside the slits is included. We have demonstrated in previous theoretical works<sup>16</sup> that these are reasonable approximations when analyzing optical properties of nanostructured good metals, like silver and gold. Moreover, within this framework, we have been able to reproduce, in semiquantitative terms, the phenomena of beaming<sup>20</sup> and enhanced transmission,<sup>21</sup> appearing for subwavelength apertures in the optical regime. We consider  $p$ -polarized light ( $E$  field pointing across the slits), for which both extraordinary transmission and electric-field enhancements have been reported. Furthermore, in this paper we concentrate on light impinging at normal incidence onto the structure.

In order to account for the nonlinear response of the material within the slits, an iterative self-consistent method is used. For this, the slit region is divided into  $N$  narrow slices,

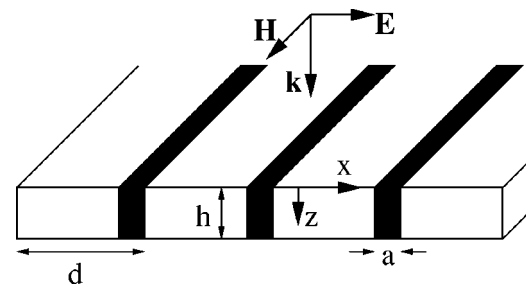


FIG. 1. Schematic view of the metallic structure under study: a metallic grating of period  $d$ , film thickness  $h$ , and slit width  $a$ . Inside the slits, we consider a Kerr nonlinear material, characterized by a Kerr coefficient,  $n_2$ . Light is considered to impinge at normal incidence with an  $E$  field pointing across the slits.

perpendicular to the  $z$  direction. For a given iteration, the magnetic field in the  $n$ th slice is expressed as

$$H_y = \frac{1}{\sqrt{a}}(A_n e^{i\sqrt{\epsilon_n} k_0 z} + B_n e^{-i\sqrt{\epsilon_n} k_0 z}), \quad (2)$$

where  $k_0$  is the wavenumber of the incident light (in vacuum),  $\epsilon_n$  is the dielectric constant in the  $n$ th slice, and  $A_n$  and  $B_n$  are the modal expansion coefficients. Within each slice, the electric field can be obtained from  $E_x = (-i/\omega\epsilon\epsilon_0) \times (\partial H_y / \partial z)$ . By matching  $E_x$  and  $H_y$ , the coefficients of the modal expansion in two consecutive strips can be related as follows,

$$\begin{pmatrix} A_{n+1} \\ B_{n+1} \end{pmatrix} = \frac{1}{2} \begin{pmatrix} C_+ \Psi_{n,-} & C_- \Psi_{n,+}^{-1} \\ C_- \Psi_{n,+} & C_+ \Psi_{n,-}^{-1} \end{pmatrix} \begin{pmatrix} A_n \\ B_n \end{pmatrix}, \quad (3)$$

with the definitions  $C_{\pm} = 1 \pm \sqrt{\epsilon_{n+1}/\epsilon_n}$ ,  $\Psi_{n,\pm} = \exp[i(\sqrt{\epsilon_n} \pm \sqrt{\epsilon_{n+1}})k_0 z_n]$ , and  $z_n$  marking the position of the interface between slices  $n$  and  $n+1$ . The modal coefficients at the entrance and exit of the slit are related through the product of the matrices corresponding to the matching of EM fields between consecutive slices. Finally, the connection with the incoming and outgoing waves outside the grating is established, obtaining the transmission and reflection coefficients for the whole structure. In the next step of the iterative procedure, a new set of  $\epsilon_n$  is obtained through Eq. (1) from the previous calculation of the  $E$  fields in the slices. For a given value of  $N$  and  $I_0$ , this linear response calculation is repeated until convergency in the set of  $\epsilon_n$  is reached. And then, for each value of  $I_0$ ,  $N$  is increased until the transmitted flux does not depend on  $N$ . Still, the described procedure does not completely specify the solution: this nonlinear system may present a multiplicity of solutions, and the transmitted flux obtained at the end may depend on the profile of  $\epsilon(z)$  that is chosen as the seed for the iterative procedure. Two choices are used in this paper: for a given incident flux we use as seeds for the iterative procedure the converged dielectric constant profiles obtained from a previous calculation for either smaller or larger incident fluxes.

Figure 2(a) renders the transmittance (total transmitted flux divided by incident flux) versus wavelength, for different values of  $I_0$  in units of  $n_2^{-1}$ . For the chosen parameters, in the linear regime [full lines in both panels (a) and (b)], the metallic grating presents two transmission peaks, that are representative of the two types of transmission resonances appearing in metallic gratings with narrow slits.<sup>10,13</sup> The peak at  $\lambda = 0.78 \mu\text{m}$ , very close to the period of the grating, corresponds to coupled surface electromagnetic modes excited at the entrance and exit interfaces of the structure, whereas the peak at  $\lambda = 1.46 \mu\text{m}$  is basically associated with a slit waveguide mode. In Fig. 2(a), the transmittance at a given wavelength has been obtained by considering the converged situation at a lower incident flux (for that particular wavelength) as the seed for the iterative scheme. As can be seen, as the incident flux is increased, the peaks shift to larger wavelengths and their magnitude decreases. In Fig. 2(b) we represent the same quantity, transmittance versus wavelength, for the same structure, but for decreasing incident fluxes. In this case, for

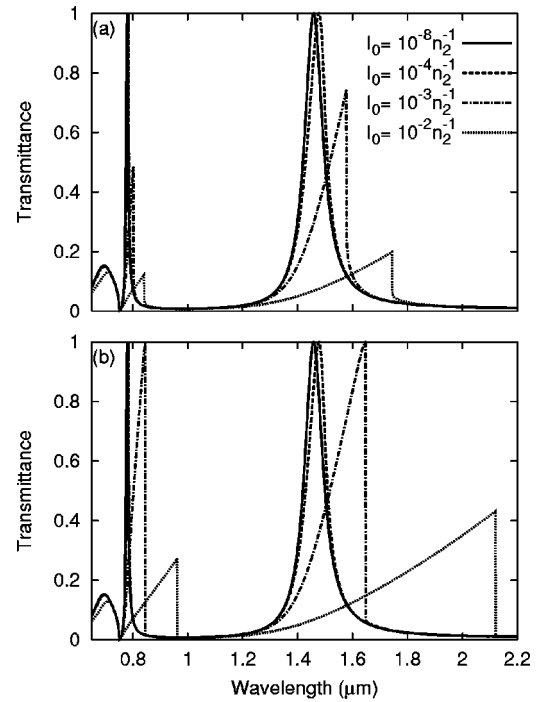


FIG. 2. Transmittance vs wavelength for different values of incident flux obtained while (a) increasing and (b) decreasing the incident flux. The parameters of the metallic gratings are:  $d=0.75$ ,  $a=0.05$ , and  $h=0.45 \mu\text{m}$ . The incident fluxes considered are (1)  $10^{-8}n_2^{-1}$ , (2)  $10^{-4}n_2^{-1}$ , (3)  $10^{-3}n_2^{-1}$ , and (4)  $10^{-2}n_2^{-1}$ .

a given wavelength, the converged dielectric constant,  $\epsilon(z)$ , is first obtained for an incident flux of  $I_{\text{max}} = 0.1n_2^{-1}$ , which is a representative value of a “high-flux” situation, and then the incident flux is decreased slowly to the value  $I_0$ . Remarkably, the transmission spectra differ for increasing and decreasing fluxes, which is a clear manifestation of **optical bistability**. Besides, for decreasing incident flux, the transmission spectra depend on the initial incident flux  $I_{\text{max}}$ . In particular, in Fig. 2(b) the transmittance peaks for incident flux  $10^{-2}n_2^{-1}$  would increase (and even reach unity) for larger values of  $I_{\text{max}}$ .

Optical bistability is better analyzed by considering the situation for a fixed wavelength. In Fig. 3(a), we show the transmitted flux as a function of  $I_0$  for  $\lambda = 1.55 \mu\text{m}$ , which is the typical wavelength used in telecommunications (and slightly larger than the wavelength of the waveguide mode in the structure under consideration in this paper). A clear bistable loop is observed at a range of incident fluxes. When increasing the incident flux [full line in Fig. 3(a)], the transmitted flux increases. At a certain incident flux (for this particular case, around  $5.4 \times 10^{-4}/n_2$ ), the transmitted flux jumps to a higher value in a discontinuous manner. By contrast, the system has a different behavior when the incident flux is decreased. The system, now in a high transmittance situation, instead of jumping back to low transmitted flux, follows the upper branch in Fig. 3(a). In this system, where losses are not included, the upper branch finishes when the ratio between the transmitted and incident flux reaches the unity. Then, the transmitted flux jumps discontinuously to a lower value. The presence of a narrow

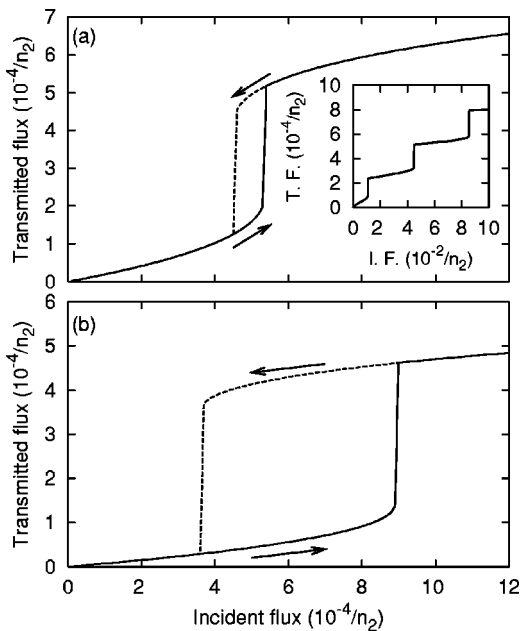


FIG. 3. Transmitted flux versus incident flux for wavelength (a)  $\lambda=1.55 \mu\text{m}$  and (b)  $\lambda=0.8 \mu\text{m}$  for a metallic grating with parameters:  $d=0.75$ ,  $a=0.05$ , and  $h=0.45 \mu\text{m}$ . The solid (dashed) lines correspond to increasing (decreasing) fluxes. In the inset of panel (a) is shown the transmitted flux vs the increasing incident flux for  $\lambda=1.55 \mu\text{m}$  for a metallic grating of the same  $a$  and  $d$  than in the panels, but with  $h=13 \mu\text{m}$ .

bistability region, such as the one illustrated in Fig. 3(a), is an interesting situation for device applications, as small changes in the incident flux would imply significant changes in the transmitted flux.

Optical bistability is also obtained associated with the transmission peak appearing at wavelengths close to the periodicity. In Fig. 3(b), we show the bistable loop obtained for a wavelength of  $\lambda=0.8 \mu\text{m}$ , just slightly larger than the period of the grating. The bistable region is wider than in the previous case, mainly due to the higher incident flux needed to jump to the upper branch when increasing the incident flux.

If the thickness of the metal film is large enough, the spectral separation between different slit waveguide modes is strongly reduced. Then, as the incident flux is increased, several resonances can participate in the transmission process, resulting in a staircase behavior of the transmitted flux versus the incident one, as can be seen in the inset of Fig. 3(a) for a metallic grating of  $h=13 \mu\text{m}$ . The curves rendered in Fig. 3 for increasing  $I_0$  are reminiscent of the transmission of light through individual pinholes in granular gold films covered with a layer of a nonlinear material,<sup>22</sup> which was discussed in terms of “photon blockade.” Notice, however, that this phenomenon is not present in our case, as we are not working in the single-photon regime.

We find that there are two characteristic EM-field patterns associated, respectively, with the lower and the upper branch of the bistability loop. At a given wavelength, the field pattern within the slits for the lower branch corresponds approximately to the field pattern obtained in the linear re-

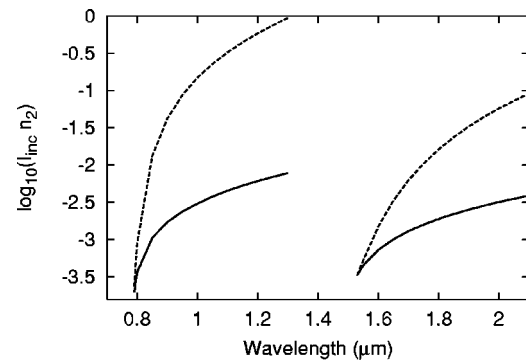


FIG. 4. Incident flux, in logarithmic scale (base 10), corresponding to the beginning (continuous line) and end (dashed line) of the first bistable region as a function of the wavelength for a metallic grating with parameters:  $d=0.75$ ,  $a=0.05$ , and  $h=0.45 \mu\text{m}$ .

sponse calculation. For this field pattern, the field intensity at the entrance and exit of the slits are different, as it corresponds to a low transmittance situation. Even in this case, the lower branch presents, close to its instability, nonlinearities. However, these nonlinearities are associated more with the change in the *average* dielectric constant inside the slit [via Eq. (1)], than with changes in the EM-field profile. The upper branch presents the field intensity pattern associated with the closest transmission resonance located at a shorter wavelength,<sup>23</sup> which is symmetric with respect to the center of the slit.

Let us now study how the width of the bistability region depends on the wavelength. In Fig. 4, we show the incident flux corresponding to the start and end of this region as a function of the wavelength. For wavelengths in the interval between  $0.79$  and  $1.53 \mu\text{m}$ , bistability is related to the shift to larger wavelengths of the peak appearing close to the period for low incident flux. The width of the bistability region increases dramatically with the wavelength. We arbitrarily terminate the curves at  $\lambda=1.3 \mu\text{m}$ , since the incident flux needed to jump to the upper branch, which corresponds to the end of the bistability region, becomes so high that our model is no longer valid. For wavelengths larger than  $1.53 \mu\text{m}$ , the first bistability region is related to the shift to larger wavelengths of the slit waveguide mode appearing approximately at  $1.46 \mu\text{m}$  at low incident flux. Notice that the bistability regions do not start exactly at the position of the linear-response transmission peaks, but at slightly larger wavelengths. It is worth pointing out that optical bistability occurs at similar incident flux levels for both resonances. This is due to the fact that, as the transmittance at peaks is approximately 100%, the *E*-field intensities *inside the slits* for different peaks have comparable maximum values. Therefore, both resonances are affected by the nonlinear response in a similar way.

Given available fluxes and Kerr nonlinear media, optical bistability should be experimentally accessible already. For instance, some polymers can present a Kerr coefficient up to  $10^{-8}$ – $10^{-9} \text{ cm}^2/\text{W}$ . These values would imply incident fluxes of the order of  $10^4$ – $10^5 \text{ W}/\text{cm}^2$  for observing bistability, for the parameters chosen in this article. For higher ratios between the lattice parameter and the slit,

given that the energy flux inside the slits increases as  $d/a$ , bistability should occur for even smaller values of the incident flux.

In summary, we have analyzed the optical response of a metallic grating with subwavelength slits containing Kerr nonlinear media by means of a self-consistent method. The nonlinear response induces changes in the transmission spectra, with shifts of the transmission peaks to larger wavelengths. In addition, transmission spectra differ for increasing and decreasing intensity. An important result is the observation of optical bistability for certain ranges of wave-

length and incident flux. The levels of optical power needed for observing these effects are attainable for typical Kerr nonlinear materials.

J.A.P. gratefully acknowledges financial support from the Ramón y Cajal Program from the Ministerio de Ciencia y Tecnología of Spain. Financial support by the Spanish MCyT under Contract Nos. MAT2002-01534 and MAT2002-00139, and by the EU-STREP Project “Surface Plasmon Photonics” (FP6-NMP4-CT-2003-505699), is gratefully acknowledged.

- 
- <sup>1</sup>S. John and N. Akozbek, Phys. Rev. Lett. **71**, 1168 (1993).  
<sup>2</sup>M. Scalora, J. P. Dowling, C. M. Bowden, and M. J. Bloemer, Phys. Rev. Lett. **73**, 1368 (1994).  
<sup>3</sup>J. W. Fleischer, M. Segev, N. K. Efremidis, and D. N. Christodoulides, Nature (London) **422**, 147 (2003).  
<sup>4</sup>E. Centeno and D. Felbacq, Phys. Rev. B **62**, R7683 (2000).  
<sup>5</sup>M. Soljacić, M. Ibanescu, S. G. Johnson, Y. Fink, and J. D. Joannopoulos, Phys. Rev. E **66**, 055601(R) (2002).  
<sup>6</sup>M. Soljacić, C. Luo, J. D. Joannopoulos, and S. Fan, Opt. Lett. **28**, 637 (2003).  
<sup>7</sup>M. F. Yanik, S. Fan, and M. Soljacić, Appl. Phys. Lett. **83**, 2739 (2003).  
<sup>8</sup>T. W. Ebbesen, H. J. Lezec, H. F. Ghaemi, T. Thio, and P. A. Wolff, Nature (London) **391**, 667 (1998).  
<sup>9</sup>U. Schröter and D. Heitmann, Phys. Rev. B **58**, 15 419 (1998).  
<sup>10</sup>J. A. Porto, F. J. García-Vidal, and J. B. Pendry, Phys. Rev. Lett. **83**, 2845 (1999).  
<sup>11</sup>H. E. Went, A. P. Hibbins, J. R. Sambles, C. R. Lawrence, and A. P. Crick, Appl. Phys. Lett. **77**, 2789 (2000).  
<sup>12</sup>E. Popov, M. Nevière, S. Enoch, and R. Reinisch, Phys. Rev. B **62**, 16 100 (2000).  
<sup>13</sup>S. Collin, F. Pardo, R. Teissier, and J. L. Pelouard, Phys. Rev. B **63**, 033107 (2001).  
<sup>14</sup>A. Barbara, P. Quémerais, E. Bustarret, and T. Lopez-Rios, Phys. Rev. B **66**, 161403(R) (2002).  
<sup>15</sup>A. Krishnan, T. Thio, T. J. Kim, H. J. Lezec, T. W. Ebbesen, P. A. Wolff, J. Pendry, L. Martin-Moreno, and F. J. Garcia-Vidal, Opt. Commun. **200**, 1 (2001).  
<sup>16</sup>F. J. García-Vidal and L. Martín-Moreno, Phys. Rev. B **66**, 155412 (2002).  
<sup>17</sup>I. I. Smolyaninov, A. V. Zayats, A. Stanishevsky, and C. C. Davis, Phys. Rev. B **66**, 205414 (2002).  
<sup>18</sup>A. M. Dykhne, A. K. Sarychev, and V. M. Shalaev, Phys. Rev. B **67**, 195402 (2003).  
<sup>19</sup>H. J. Lezec, A. Degiron, E. Devaux, R. A. Linke, L. Martin-Moreno, F. J. Garcia-Vidal, and T. W. Ebbesen, Science **297**, 820 (2002).  
<sup>20</sup>L. Martin-Moreno, F. J. Garcia-Vidal, H. J. Lezec, A. Degiron, and T. W. Ebbesen, Phys. Rev. Lett. **90**, 167401 (2003).  
<sup>21</sup>F. J. Garcia-Vidal, H. J. Lezec, T. W. Ebbesen, and L. Martin-Moreno, Phys. Rev. Lett. **90**, 213901 (2003).  
<sup>22</sup>I. I. Smolyaninov, A. V. Zayats, A. Gungor, and C. C. Davis, Phys. Rev. Lett. **88**, 187402 (2002).  
<sup>23</sup>This occurs for  $\chi^{(3)} > 0$ . For  $\chi^{(3)} < 0$ , the field pattern would be corresponding to the closest transmission resonance at larger wavelengths.